Asian Journal of Pharmaceutical Sciences 14 (2019) 86–94

Available online at www.sciencedirect.com

ScienceDirect

journal homepage: www.elsevier.com/locate/AJPS

Original Research Paper

Development of PLGA micro- and nanorods with high capacity of surface ligand conjugation for enhanced targeted delivery

Jiafu Cao[a,1], *Jin-Seok Choi*[a,b,1], *Murtada A. Oshi*[a], *Juho Lee*[a], *Nurhasni Hasan*[a], *Jihyun Kim*[a,c], *Jin-Wook Yoo*[a,*]

[a] *College of Pharmacy, Pusan National University, Busan 46241, South Korea*
[b] *Department of Medical Management, Chodang University, Muan-gun 58530, South Korea*
[c] *College of Nanoscience & Nanotechnology, Pusan National University, Busan 46241, South Korea*

ARTICLE INFO

Article history:
Received 21 May 2018
Revised 22 August 2018
Accepted 30 August 2018
Available online 24 September 2018

Keywords:
Particle shape
PLGA nanoparticles
Film-stretching method
Surface modification
Targeted drug delivery

ABSTRACT

Particle shape has been recognized as one of the key properties of nanoparticles in biomedical applications including targeted drug delivery. Targeting ability of shape-engineered particles depends largely on targeting ligands conjugated on the particle surface. However, poor capacity for surface ligand conjugation remains a problem in anisotropic nanoparticles made with biodegradable polymers such as PLGA. In this study, we prepared anisotropic PLGA nanoparticles with abundant conjugatable surface functional groups by a film stretching-based fabrication method with poly (ethylene-alt-maleic acid) (PEMA). Scanning electron microscopy images showed that microrods and nanorods were successfully fabricated by the PEMA-based film stretching method. The presence of surface carboxylic acid groups was confirmed by confocal microscopy and zeta potential measurements. Using the improved film-stretching method, the amount of protein conjugated to the surface of nanorods was increased three-fold. Transferrin-conjugated, nanorods fabricated by the improved method exhibited higher binding and internalization than unmodified counterparts. Therefore, the PEMA-based film-stretching system presented in this study would be a promising fabrication method for non-spherical biodegradable polymeric micro- and nanoparticles with high capacity of surface modifications for enhanced targeted delivery.

* Corresponding author. College of Pharmacy, Pusan National University, Busan 46241, Republic of Korea. Tel: +82 51 5102807
E-mail address: jinwook@pusan.ac.kr (J.-W. Yoo).
[1] Both the authors contributed equally to this work.
Peer review under responsibility of Shenyang Pharmaceutical University.

https://doi.org/10.1016/j.ajps.2018.08.008

1. Introduction

Over the past few decades, particulate systems such as microparticles (MPs) and nanoparticles (NPs) have been extensively studied for biomedical applications including targeted drug delivery, imaging, and diagnostics [1–4]. In designing the MPs and NPs, a majority of studies has focused on the particle size, surface chemistry, and material composition to control particle properties [5–9]. In recent years, the particle shape has emerged as a critical parameter that modulates an interplay between a particle and a biological milieu [10,11]. In this regard, attention has been given to the use of non-spherical shapes in the design of drug delivery carriers as a strategy to overcome certain limitations associated with spherical systems. In particular, shapes inspired by the diverse, evolutionarily conserved shapes of pathogens and cells are being used to evaluate the effects of carrier shapes on cellular uptake, *in vivo* transport, and organ distribution [12].

Non-spherical particles such as rods and disk have been shown to enable superior biological performance compared to their spherical counterparts. Several theoretical and *in vitro* models have predicted increased margination of non-spherical particles compared to spherical particles to blood vessel walls due to hydrodynamic interactions that propel non-spherical particles towards the wall during blood flow [13,14]. In addition, non-spherical particles showed reduced immune clearance as compared to spherical ones [15]. Other unique properties of non-spherical particles include their binding ability to target cells and rapid internalization, compared with spherical ones [16]. Non-spherical particles also exhibited longer blood-circulation times and improved tumor accumulation in solid tumors in comparison with their spherical counterparts [17–19].

Given the aforementioned unique properties of non-spherical shapes, several different shape-engineering techniques have been developed; these methods include non-wetting templates, microfluidic systems, template assemblies, and a film stretching [20–22]. Among the fabrication methods, the film stretching method has been considered a simple, versatile, inexpensive, and high-throughput method [23,24]. In the film stretching method, different non-spherical shapes can be fabricated by immobilization of polymeric particles in a polyvinyl alcohol (PVA) film, heating the film above the glass transition temperature of polymeric particles, followed by stretching to deform the particles. The film stretching method has been widely used for the investigation of shape effects on drug delivery applications such as particle-cell interactions, drug release, vaccine delivery, cellular trafficking [24–26].

Recently, shape effect on targeting efficacy of NPs in the presence of surface ligands has gained much attention. Several studies found that interplay between shape and surface targeting ligand in NP is of importance in particle-cell interaction including NP binding to cells and cellular uptake [27]. Barua et al. demonstrated that trastuzumab-coated rod-shaped polystyrene NPs exhibited higher specific and lower nonspecific uptake in breast cancer cells than did spherical counterparts [28]. In another study, Poornima et al. demonstrated that the shape of ligand-displaying nanoparticles enhances the specificity of endothelial targeting [29]. In the studies, polystyrene-based nanoparticles were used to fabricate non-spherical NPs by a PVA film stretching method and the targeting ligands were coated on the surfaces by simple physical adsorption. However, the polystyrene is neither biodegradable nor biocompatible, thus limiting clinical applications. One promising alternative to polystyrene is poly (lactic-co-glycolic acid) (PLGA), an FDA-approved biodegradable polymer, that has long been used for drug delivery due to its biocompatibility, safety for human use, and ability to release encapsulated drugs in a controlled manner [30]. However, physical adsorption of targeting ligands to the negatively charged PLGA particles is inefficient due to the difficulties associated with controlling the molecular orientation of physically bound ligands [31]. Moreover, use of PVA film for the stretching process results in the residual PVA on the surface of PLGA NPs, which represents a barrier against the covalent ligand conjugation because it shields the functional group of PLGA (i.e. carboxylic group) [32,33].

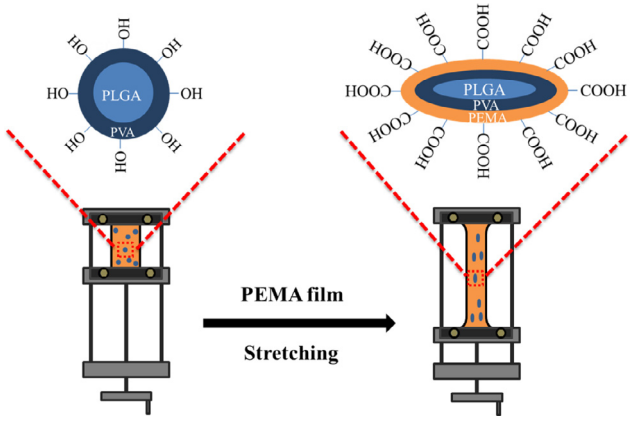

Fig. 1 – Fabrication of surface-conjugatable, microrods and nanorods by PEMA film stretching.

In this study, surface-conjugatable non-spherical PLGA NPs with a sufficient number of carboxylic acids on the surface were developed. To increase the number of carboxylic acid groups immobilized to the surface of non-spherical PLGA particles, the PVA film was replaced with poly (ethylene-alt-maleic acid; PEMA) film bearing carboxylic acid side chains (Fig. 1). Rod-shaped PLGA MPs (microrods) and NPs (nanorods) were fabricated by the PEMA film-based stretching method. Two model ligands, fluorescein isothiocyanate (FITC)-conjugated albumin and transferrin (Tf), were conjugated on the particle surfaces. The presence of surface carboxylic acid groups was determined by confocal microscopy and zeta potential measurements. Cellular uptake of Tf-conjugated nanorods by KB human carcinoma cells was also evaluated.

2. Materials and methods

2.1. Materials

PLGA (50:50 DLG 5E, intrinsic viscosity 0.47 dL/g; PLGA-ester (with ester terminated end) and 50:50 DLG 4A, in-

trinsic viscosity 0.38 dL/g; PLGA-acid (with acid terminated end)) was purchased from Lakeshore Biomaterials (Birmingham, AL, USA). PVA, PEMA, N-hydroxysuccinimide (NHS), N-(3-dimethylaminopropyl)-N′-ethylcarbodiimide hydrochloride (EDC), and FITC-albumin were purchased from Sigma-Aldrich (St. Louis, MO, USA). Tf was purchased from Athens Research & Technology (Athens, GA, USA). All other chemicals used were of analytical grade.

2.2. Particle preparation

PLGA nanospheres and microspheres were fabricated by the oil-in-water emulsion solvent-evaporation method [34]. For nanospheres preparation, 50 mg of PLGA was dissolved in 5 ml of methylene chloride. For the uptake study, 0.1 mg of coumarin-6 (C6) was added to this solution. The organic phase was mixed with 1% (w/v) PVA or 1% (w/v) PEMA solution (20 ml) and then was emulsified using a probe sonicator (KFS-300N ultrasonic processor, Korea Process Technology, Korea) at a power of 100 W for 1 min in an ice bath. The resultant emulsion was mechanically stirred for 3 h at 500 rpm in a fume hood to remove residual organic solvents. Nanospheres were collected by centrifugation at 20 000 × g for 1 h and then washed three times with double-distilled water. For microspheres preparation, 100 mg of PLGA was dissolved in 3 ml of methylene chloride. This organic phase was mixed with 1% (w/v) PVA or 1% (w/v) PEMA solution (20 ml) and then emulsified for 5 min, using a homogenizer with a stirring rate of 2,000 rpm in an ice bath. The resultant emulsion was mechanically stirred for 3 h at 500 rpm in a fume hood to remove residual organic solvents. Microspheres were collected by centrifugation at 200 × g for 30 min and were washed 3 times using double-distilled water.

2.3. Surface-conjugatable microrods and nanorods preparation

Microrods were prepared by the previously reported film-stretching method with some modification (Fig. 1) [23]. To fabricate the stretching film, 10% (w/v) PVA and 10% (w/v) PEMA were initially blended at different ratios, after which PLGA-acid/PVA (polymer: PLGA-acid, surfactant: PVA), PLGA-acid/PEMA (polymer: PLGA-acid, surfactant: PEMA), PLGA-ester/PVA (polymer: PLGA-ester, surfactant: PVA), and PLGA-ester/PEMA (polymer: PLGA-ester, surfactant: PEMA) were added to the mixtures. The film was dried on square dishes for 15 h in an incubator at 37 °C. The dried film was cut into 2.5 × 5 cm^2 sections and mounted on a custom axial-made stretcher. The film was stretched in mineral oil at 58–64 °C at a rate of 0.5–1.0 mm/s. After stretching, each film was stored in cold mineral oil for 5 min to lower the temperature and washed with ethyl ether to remove residual oil. Each film was then dissolved in double-distilled water and the stretched particles were collected by centrifuging for 1 h at 200 × g, followed by washing 5 times with double-distilled water. Nanorods were also prepared according to the film-stretching method (80% PEMA film) with the exception that the nanoparticles were added to the mixtures to make the film.

2.4. Immobilization of Tf and FITC-albumin to the surfaces of microrods and nanorods

Tf and FITC-albumin were conjugated onto the surfaces of microrods or nanorods using carbodiimide chemistry. Particles (20 mg) were dispersed in 5 ml of 2-(N-morpholino)ethanesulfonic acid (MES) buffer (0.1 M, pH 5.5) and then reacted with 200 µl of EDC (10 mg/ml) and 200 µl of NHS (10 mg/ml) for 2 h. Excess unreacted EDC and NHS were removed by 3 rounds of washing with MES buffer and centrifugation. The particles with activated carboxyl groups were dispersed in 6 ml of phosphate-buffered saline (PBS, pH 7.4), and then reacted with 300 µl of FITC-albumin (1.0 mg/ml in PBS) or Tf (10.0 mg/ml in PBS) for 4 h in the dark at room temperature. Excess unconjugated Tf and FITC-albumin were removed by three rounds of centrifugation at 20,000 × g for 30 min in PBS buffer. Tf and FITC-albumin adsorption to particle surfaces were performed as described for the conjugation experiments, except that MES buffer was used instead of the EDC and NHS solutions.

2.5. Determination of Tf and FITC-albumin on the surfaces of microrods and nanorods

The conjugation of FITC-albumin to the surfaces of microrods was visualized by confocal microscopy (Fluoview FV10i, Olympus, Tokyo, Japan). The fluorescence intensities of FITC-albumin-conjugated nanorods were measured on a multimode microplate reader (TriStar LB 941, Berthold Technologies, Bad Wildbad, Germany), using excitation and emission wavelengths of 460 nm and 540 nm, respectively. Unconjugated free Tf proteins in the supernatants were quantified using a BCA Assay Kit (Fisher Scientific, Waltham, MA, USA). The quantities of Tf on the nanorods surfaces were calculated by subtracting the free protein in the supernatants from the original amount added.

2.6. Scanning-electron microscopy (SEM)

Microrods and nanorods were characterized by field-emission SEM (FE-SEM, S4800, Hitachi, Japan). The particles were dispersed in double-distilled water, dropped onto a carbon tape, and then dried in a fume hood and desiccator. The carbon tapes with PLGA particles were coated with platinum for 2 min under a vacuum. The samples were viewed by FE-SEM, under acceleration voltages of 5 kV and 35 kV. Particle sizes were measured using ImageJ software (NIH, Bethesda, MD, USA; $n = 100$).

2.7. Zeta potential

The zeta potential distribution was measured using a Zetasizer Nano ZS (Malvern Instruments, Malvern, UK). Samples were diluted in double-distilled water and placed in a zeta cell. The average of three measurements of each sample was used to derive the average zeta potential.

2.8. Confocal microscopy

Human epidermoid cancer KB cells were grown in RPMI 1640supplemented with 10% (v/v) fetal bovine serum and an-

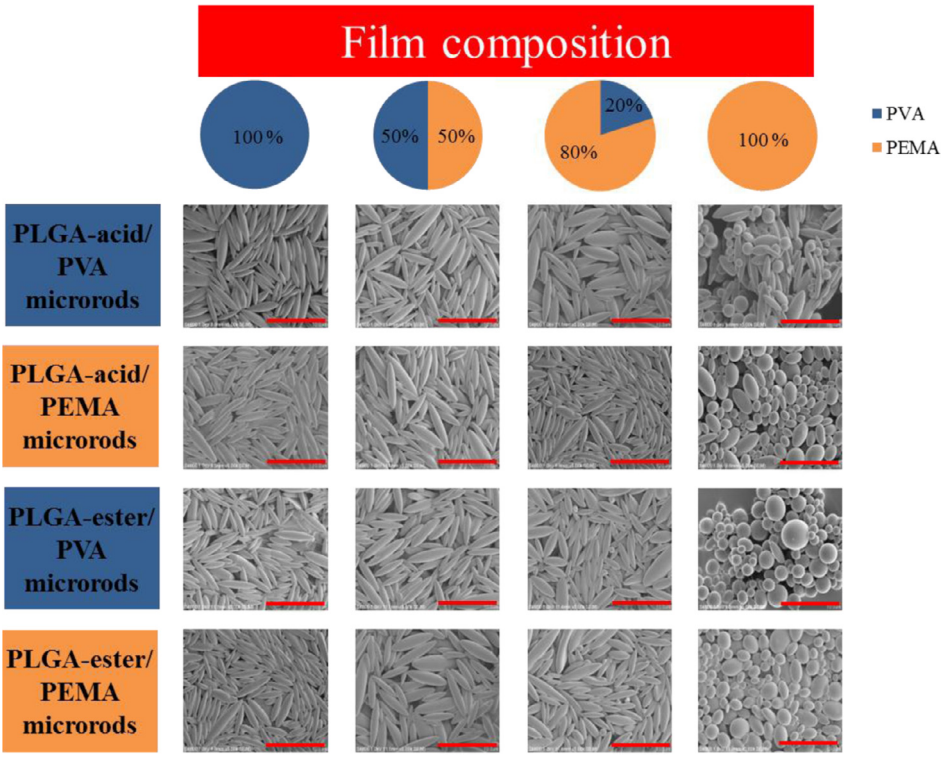

Fig. 2 – SEM images of microrods fabricated using different proportions of PEMA and PVA with four differently formulated microspheres. The scale bars are 10 µm.

tibiotics (100 IU/ml of penicillin G sodium and 100 µg/ml of streptomycin sulfate). Cells were maintained in an incubator supplied under a humidified 5% CO_2/95% air atmosphere at 37 °C. KB cells were seeded on cover glasses in a 6-well plate at an initial density of 5×10^4 cells /well. The cells were incubated with Tf-conjugated and C6-loaded nanorods fabricated using PVA and PEMA. After 2 h, the cells were washed several times with cold PBS and fixed with 4% paraformaldehyde for 10 min. The cells were washed twice with cold PBS and then incubated with 0.1% Triton X-100 in 0.2 N NaOH for 5 min. The nuclei were stained with 4′,6-diamidino-2-phenylindole (DAPI; 2 µg/ml) for 5 min, the cells fixed with Permount Mounting Medium (Fisher Scientific), and then observed by confocal microscopy (Fluoview FV10i).

2.9. *Statistical analysis*

Statistical analysis was performed using the paired *t*-test in SigmaPlot 12.0 (SYSTAT, Inc., Chicago, IL, USA). Results are expressed as means ± SD. Statistical significance was accepted for P values < 0.05.

3. Results and discussion

3.1. *Preparation of PLGA microrods and nanorods*

The purpose of this study was to develop a modifiable surface of non-spherical biodegradable NPs prepared by a film stretching method for use as a drug delivery system. Introduction of a functional group, such as a carboxylate group, to non-spherical particles made by the conventional PVA film stretching method, has been limited due to the residual PVA on the surface. In this study, however, we utilized the property of residual film composition to fabricate a surface-conjugatable non-spherical NPs. PEMA has been used as a surfactant during particles fabrication to increase the number of carboxyl groups on the surface of PLGA particles for surface modification [35]. If PEMA was used as a stretching film to fabricate non-spherical NPs, non-spherical NPs with abundant conjugatable surface functional groups can be fabricated. Fabrication of surface-modifiable, microrods and nanorods using PEMA film was illustrated in Fig. 1. In order to see whether we can increase the amount of carboxyl groups on the surface of microrods by increasing the amount of carboxyl groups on the surface of microspheres, four different microspheres (PLGA-acid/PVA, PLGA-acid/PEMA, PLGA-ester/PVA and PLGA-ester/PEMA) were fabricated using the oil-in-water emulsion solvent-evaporation method. It is worth to note that there are two types of PLGA end groups (acid-end and ester-end). Unlike PLGA-ester, PLGA-acid has end carboxylic groups, which could potentially increase the availability of carboxylic groups in the surface of non-spherical particles after the film stretching [36]. Likewise, we also compared two surfactants, PVA and PEMA. As compared to PVA, PEMA has carboxylic groups, thus it may also increase the availability of carboxylic groups at the final non-spherical particles. Four different microspheres were converted to microrods by the film stretching method and their aspect ratios were evaluated.

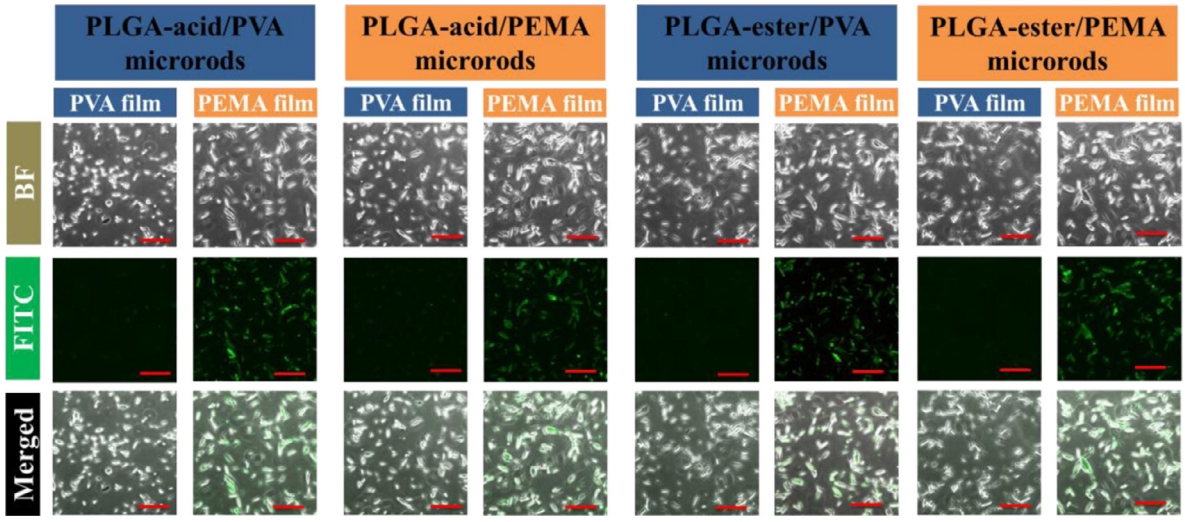

Fig. 3 – Confocal images of microrods with surface-conjugated FITC-albumin. Scale bars in bright field (BF) images correspond to 5 μm.

Fig. 2 shows the SEM images of microrods fabricated with different ratios of PEMA and PVA with four differently formulated microspheres. First, the microrods were fabricated by the 100% PVA film (called hereafter PVA film) as a control for comparative studies. Four PLGA microrods with the same aspect ratio (rod length divided by diameter) of 5 were observed by using PVA film. The PLGA and surfactants types have no effect on the aspect ratio of microrods. Second, we attempted to fabricate microrods using 100% PEMA film; however, the use of 100% PEMA film resulted in an incomplete stretching as determined by SEM in Fig. 2, indicating the difficulty in fabricating microrods using 100% PEMA film. It could be because the force holding the particles in the PEMA film was lower than that operating in the PVA film. At last, PEMA was blended with PVA at different ratios. We found that 50% PEMA film and 80% PEMA film resulted in microrods with similar aspect ratios with PVA film, indicating that successful fabrication of microrods. For further studies, we selected the 80% PEMA film (called hereafter PEMA film) because high carboxylate group densities are required on the particle surface for modification of the nanorods by ligand conjugation.

3.2. *Determination of carboxyl groups on the surface of microrods*

For detection of the surface carboxyl groups, we conjugated FITC-albumin to the surface of microrods using a carbodiimide chemistry-based method. Using EDC and NHS as chemical crosslinkers, the surface carboxyl groups of the PLGA microrods were activated so that they could bind covalently to the terminal amine group of FITC-albumin. The amount of FITC- albumin coating on the surface of microrods was assessed by monitoring the fluorescence changes in confocal microscopy. Fig. 3 shows confocal images of microrods with FITC-albumin conjugated to their surfaces. We fabricated 8 kinds of microrods using PVA film and PEMA film. The FITC channel revealed the green fluorescence of FITC-albumin. The microrods fabricated by using PEMA film exhibited high fluorescence levels, whereas none of the microrods fabricated using the PVA film exhibited fluorescence. PLGA-acid and PEMA surfactant did not increase the fluorescence levels, indicating using PLGA-acid as a polymer and PEMA as a surfactant do not increase the availability of surface carboxyl groups. These results demonstrated that, when using PEMA film, we could fabricate microrods with surface carboxyl groups regardless of end groups of PLGA and surfactant types.

3.3. *Zeta potentials*

We analyzed the zeta potentials of microrods using a Zetasizer Nano ZS system to further confirm the presence of surface carboxyl groups on the microrods. It is worth noting that the terminal carboxyl groups on the surface decrease the zeta potentials. As shown in Fig. 4, when PEMA was used as a surfactant to prepare microspheres, the zeta potential of microspheres was nearly −40 mV. Whereas the zeta potential of microspheres prepared with PVA as a surfactant was approximately −20 mV. The zeta potential of microspheres fabricated using PLGA-ester was higher than those fabricated using PLGA-acid. In general, surfactant-free PLGA NPs exhibit a negative zeta potential (−49 mV) due to the presence of terminal carboxylic groups in PLGA [37]. A residual surfactant on the particle surface can affect the zeta potential. Microspheres prepared using PVA as a surfactant show a low negative charge due to hydroxyl groups (-OH) of PVA, whereas ones prepared using PEMA show high negative charge due to carboxyl groups (-COOH) of PEMA [38]. The PLGA type had little effect on the zeta potential of microspheres although the value obtained using PLGA-acid was somewhat higher than that obtained using PLGA-ester. After film-stretching using PVA film, the zeta potential of all of the microrods became approximately −20 mV; however, the zeta potential of microrods after film-stretching with PEMA film was nearly −40 mV. We found that the factor that determines the zeta potential of mi-

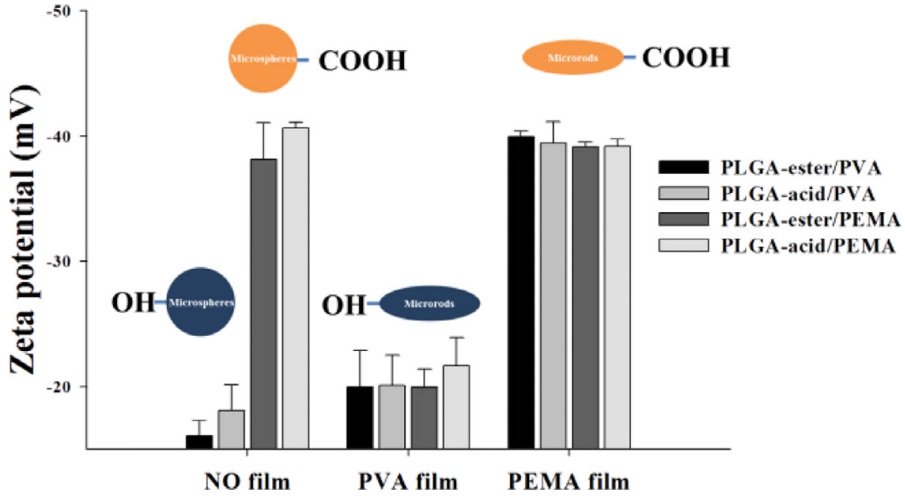

Fig. 4 – The surface charge of PLGA MPs. Results are expressed as the means ± SD ($n = 3$).

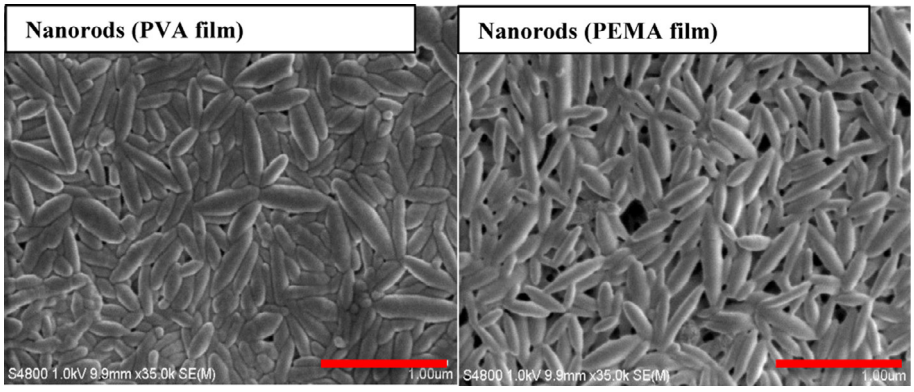

Fig. 5 – SEM images of nanorods. The dimensions of nanorods fabricated using PVA film were 373.2 ± 97.5 nm (length) by 98.7 ± 18.5 nm (width), while those of nanorods fabricated using PEMA film were 385.8 ± 88.2 nm (length) by 105.9 ± 25.7 nm (width). The scale bars are 1 μm.

Table 1 – Physicochemical characteristics of nanorods.

Formulation	Particle dimension (length × width, nm)	Zeta potential (mV)
Nanorods (PVA film)	373.2 ± 97.5 × 98.7 ± 18.5	−18.5 ± 0.9
Nanorods (PEMA film)	385.8 ± 88.2 × 105.9 ± 25.7	−38.5 ± 0.5

Results are presented as the means ± SD ($n = 3$)

crorods was the film composition during particle stretching, not the type of PLGA nor surfactants used during the microsphere preparation.

3.4. *Characterization of nanorods*

PLGA NPs have been used as drug delivery systems in various biomedical applications involving cancer, inflammation, and other diseases, because of their versatility in terms of biocompatibility, drug-loading ability, and controlled-drug release [39]. A wide range of pharmaceuticals such as hydrophilic or hydrophobic small molecules or macromolecules has been delivered via PLGA NPs [40]. By the PEMA-based film stretching method, surface-modifiable nanorods were also successfully fabricated. Fig. 5 shows SEM images of nanorods fabricated using both PVA film and PEMA film. SEM images showed that the nanorods exhibited a regular rod shape and uniform size without any noticeable pinholes or cracks and with a narrow size distribution. The properties of nanorods are summarized in Table 1. The mean size of the nanorods was 373.2 nm × 98.7 nm for PVA film and 385.8 nm × 105.9 nm for PEMA film, resulting in an average aspect ratio of 4. Their mean zeta potentials were −19.5 and −38.5 mV, respectively, which are consistent with results from microrods.

3.5. *Determination of Tf and FITC-albumin on the surfaces of nanorods*

To determine the feasibility of nanorods for surface modification, the capacity for protein immobilization on the surface of nanorods fabricated using either PVA film or PEMA film was tested using Tf and FITC-albumin. Two strategies for attaching proteins to nanorods were used: conjugation and adsorption. Fig. 6A shows the amount of surface-conjugated Tf

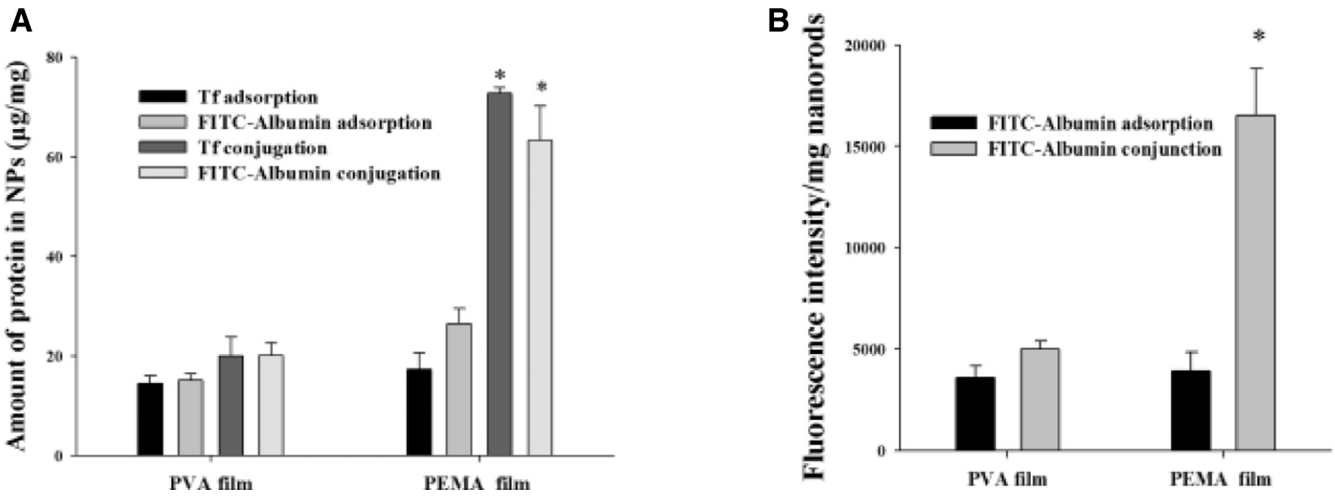

Fig. 6 – Amount of protein on the particle surface (A) and fluorescence intensities (B) of nanorods fabricated using different film types. The results are expressed as the mean ± SD ($n = 3$). *$P < 0.05$ vs. nanorods fabricated using PVA film.

and FITC-albumin on nanorods. The amount of protein conjugated to the surface of nanorods generated using PEMA film was ~70 μg/mg NPs. However, when PVA film was used, the amount of Tf and protein on the surface of nanorods was only ~20 μg/mg NPs regardless of binding methods. Fig. 6B shows the fluorescence intensities of nanorods fabricated using different film types. The fluorescence came from FITC-albumin, which was conjugated on the surface of nanorods. Nanorods fabricated using PEMA film show over 3-fold higher fluorescence intensities than ones fabricated using PVA film, which is consistent with result of the amount of protein on the nanorods, indicating that the Tf and FITC-albumin on the surface of nanorods fabricated using PVA were not conjugated but merely adsorbed, proving that residual PVA from PVA film is a potential barrier against ligand conjugation to the particle surface. Thus, PVA film is not appropriate for surface ligand conjugation of non-spherical particles. Overall, PEMA film is the optimal film for fabricating non-spherical particles with a high capacity of surface ligand conjugation.

3.6. *Cellular uptake*

The delivery of drugs into specific cell types can significantly reduce drug toxicity and increase their therapeutic effects [41,42]. Various targeting ligands have been utilized to increase the intracellular uptake of NPs [43]. Among them, Tf is a widely used targeting ligand for tumor-targeted delivery. The extent of the cellular uptake of nanorods conjugated with the Tf was investigated in KB cells which overexpresses Tf receptors. Fig. 7 shows the cellular-uptake of Tf-conjugated coumarin-6-loaded nanorods (fabricated using PVA and PEMA) in KB cells. The blue fluorescence by the nuclear dye DAPI, which did not co-localize with green fluorescence representing the nanorods internalized to the cytoplasm. Nanorods fabricated using PEMA film exhibited even higher intracellular accumulation as compared to those fabricated using PVA film. The cellular uptake of NPs can be viewed as a two-step process: a binding step on the cell membrane and an internalization step [44] Interactions between ligand-modified NPs and cellular receptors depend on the molecular orientation and ligand density on the NPs surface. The nanorods fabricated using PEMA film have more ligands conjugated to the surface of nanorods. As shown in the Fig. 7, Tf-nanorods (PEMA film) have strong binding

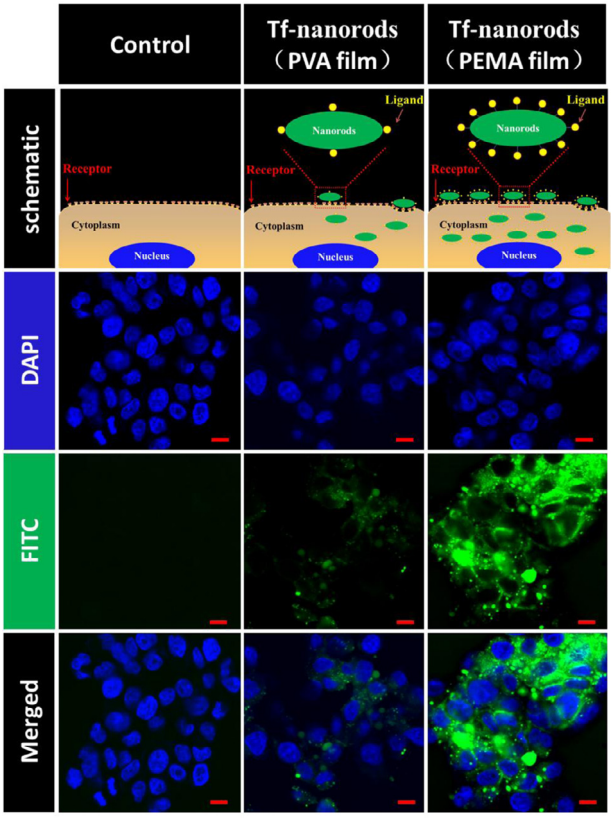

Fig. 7 – Confocal microscopy image of cellular-uptake studies of Tf-conjugated, coumarin-6-loaded, nanorods (fabricated using PVA and PEMA) in KB cells after a 2-h incubation. The scale bars are 10 μm.

affinity to the Tf receptor on the cell membrane compare to Tf-nanorods (PVA film) because of multiple receptor-ligand complexes at the cell surface. Receptor-mediated endocytosis has been shown to facilitate and promote particle penetration into cells when Tf was conjugated on the surface of NPs [45]. These results demonstrated the advantage of the surface-modifiable nanorods in targeted drug delivery.

4. Conclusion

In this study, surface-conjugatable, micro- and nanorods were successfully fabricated by the PEMA-based film-stretching method. The film type was identified as the key factor facilitating the fabrication of surface-conjugatable non-spherical particles. FITC-albumin and Tf were successfully conjugated to the surfaces of nanorods, demonstrating that the system has the ability to enhance surface ligand conjugation. Furthermore, Tf-conjugated nanorods fabricated using PEMA film exhibited higher binding and cellular uptake in KB cell than those fabricated using PVA film. Therefore, the PEMA-based film-stretching system presented in this study would be a promising fabrication method for non-spherical biodegradable polymeric micro- and nanoparticles with high capacity of surface modifications for enhanced targeted delivery.

Declaration of interest

The authors report no conflicts of interest. The authors alone are responsible for the content and writing of this article.

Acknowledgments

This research was supported by a grant from the Korean Healthcare Technology R&D Project, Ministry for Health and Welfare Affairs, Republic of Korea (HI15C2558).

REFERENCES

[1] Park O, Yu G, Jung H, Mok H. Recent studies on micro-/nano-sized biomaterials for cancer immunotherapy. J Pharm Investig 2017;47(1):11–18.
[2] Mohtashamian S, Boddohi S. Nanostructured polysaccharide-based carriers for antimicrobial peptide delivery. J Pharm Investig 2017;47(2):85–94.
[3] Choi JH, Lee YJ, Kim D. Image-guided nanomedicine for cancer. J Pharm Investig 2017;47(1):51–64.
[4] Sarisozen C, Pan J, Dutta I, Torchilin VP. Polymers in the co-delivery of siRNA and anticancer drugs to treat multidrug-resistant tumors. J Pharm Investig 2017;47(1):37–49.
[5] Albanese A, Tang PS, Chan WC. The effect of nanoparticle size, shape, and surface chemistry on biological systems. Annu Rev Biomed Eng 2012;14:1–16.
[6] Lee SS, Lee YB, Oh IJ. Cellular uptake of poly (dl-lactide-co-glycolide) nanoparticles: effects of drugs and surface characteristics of nanoparticles. J Pharm Investig 2015;45(7):659–67.
[7] Yoo JW, Irvine DJ, Discher DE, Mitragotri S. Bio-inspired, bioengineered and biomimetic drug delivery carriers. Nat Rev Drug Discov 2011;10(7):521–35.
[8] Yoo JW, Doshi N, Mitragotri S. Adaptive micro and nanoparticles: temporal control over carrier properties to facilitate drug delivery. Adv Drug Deliv Rev 2011;63(14):1247–56.
[9] Hoang NH, Lim C, Sim T, Oh KT. Triblock copolymers for nano-sized drug delivery systems. J Pharm Investig 2017;47(1):27–35.
[10] Mitragotri S. In drug delivery, shape does matter. Pharm Res 2009;26(1):232–4.
[11] Champion JA, Katare YK, Mitragotri S. Particle shape: a new design parameter for micro-and nanoscale drug delivery carriers. J Control Release 2007;121(1):3–9.
[12] Agarwal R, Singh V, Jurney P, Shi L, Sreenivasan S, Roy K. Mammalian cells preferentially internalize hydrogel nanodiscs over nanorods and use shape-specific uptake mechanisms. Proc Natl Acad Sci USA 2013;110(43):17247–52.
[13] Gavze E, Shapiro M. Motion of inertial spheroidal particles in a shear flow near a solid wall with special application to aerosol transport in microgravity. J Fluid Mech 1998;371:59–79.
[14] Thompson AJ, Mastria EM, Eniola-Adefeso O. The margination propensity of ellipsoidal micro/nanoparticles to the endothelium in human blood flow. Biomaterials 2013;34(23):5863–71.
[15] Florez L, Herrmann C, Cramer JM, et al. How shape influences uptake: interactions of anisotropic polymer nanoparticles and human mesenchymal stem cells. Small 2012;8(14):2222–30.
[16] Gratton SE, Ropp PA, Pohlhaus PD, et al. The effect of particle design on cellular internalization pathways. Proc Natl Acad Sci USA 2008;105(33):11613–18.
[17] Geng Y, Dalhaimer P, Cai S, et al. Shape effects of filaments versus spherical particles in flow and drug delivery. Nat Nanotechnol 2007;2(4):249–55.
[18] Park JH, von Maltzahn G, Zhang L, et al. Systematic surface engineering of magnetic nanoworms for *in vivo* tumor targeting. Small 2009;5(6):694–700.
[19] Janát-Amsbury M, Ray A, Peterson C, Ghandehari H. Geometry and surface characteristics of gold nanoparticles influence their biodistribution and uptake by macrophages. Eur J Pharm Biopharm 2011;77(3):417–23.
[20] Rolland JP, Maynor BW, Euliss LE, Exner AE, Denison GM, DeSimone JM. Direct fabrication and harvesting of monodisperse, shape-specific nanobiomaterials. J Am Chem Soc 2005;127(28):10096–100.
[21] Xu S, Nie Z, Seo M, et al. Generation of monodisperse particles by using microfluidics: control over size, shape, and composition. Angew Chem 2005;117(5):734–8 .
[22] Mathaes R, Winter G, Besheer A, Engert J. Non-spherical micro-and nanoparticles: fabrication, characterization and drug delivery applications. Expert Opin Drug Deliv 2015;12(3):481–92.
[23] Champion JA, Katare YK, Mitragotri S. Making polymeric micro-and nanoparticles of complex shapes. Proc Natl Acad Sci USA 2007;104(29):11901–4.
[24] Meyer RA, Meyer RS, Green JJ. An automated multidimensional thin film stretching device for the generation of anisotropic polymeric micro-and nanoparticles. J Biomed Mater Res A 2015;103(8):2747–57.
[25] Kumar S, Anselmo AC, Banerjee A, Zakrewsky M, Mitragotri S. Shape and size-dependent immune response to antigen-carrying nanoparticles. J Control Release 2015;220:141–8.
[26] Fan JB, Song Y, Li H, Jia JP, Guo X, Jiang L. Controllable drug release and effective intracellular accumulation highlighted

by anisotropic biodegradable PLGE nanoparticles. J Mater Chem B 2014;2(25):3911–14.
[27] Banerjee A, Qi J, Gogoi R, Wong J, Mitragotri S. Role of nanoparticle size, shape and surface chemistry in oral drug delivery. J Control Release 2016;238:176–85.
[28] Barua S, Yoo JW, Kolhar P, Wakankar A, Gokarn YR, Mitragotri S. Particle shape enhances specificity of antibody-displaying nanoparticles. Proc Natl Acad Sci USA 2013;110(9):3270–5.
[29] Kolhar P, Anselmo AC, Gupta V, et al. Using shape effects to target antibody-coated nanoparticles to lung and brain endothelium. Proc Natl Acad Sci USA 2013;110(26):10753–8.
[30] Choi JS, Seo K, Yoo JW. Recent advances in PLGA particulate systems for drug delivery. J Pharm Investig 2012;42(3):155–63.
[31] Patil S, Sandberg A, Heckert E, Self W, Seal S. Protein adsorption and cellular uptake of cerium oxide nanoparticles as a function of zeta potential. Biomaterials 2007;28(31):4600–7.
[32] Sahoo SK, Panyam J, Prabha S, Labhasetwar V. Residual polyvinyl alcohol associated with poly (D, L-lactide-co-glycolide) nanoparticles affects their physical properties and cellular uptake. J Control Release 2002;82(1):105–14.
[33] Eniola AO, Rodgers SD, Hammer DA. Characterization of biodegradable drug delivery vehicles with the adhesive properties of leukocytes. Biomaterials 2002;23(10):2167–77.
[34] Cao J, Naeem M, Noh JK, Lee EH, Yoo JW. Dexamethasone phosphate-loaded folate-conjugated polymeric nanoparticles for selective delivery to activated macrophages and suppression of inflammatory responses. Macromol Res 2015;23(5):485–92.
[35] Keegan ME, Falcone JL, Leung TC, Saltzman WM. Biodegradable microspheres with enhanced capacity for covalently bound surface ligands. Macromolecules 2004;37(26):9779–84.
[36] Sunshine JC, Perica K, Schneck JP, Green JJ. Particle shape dependence of CD8+ T cell activation by artificial antigen presenting cells. Biomaterials 2014;35(1):269–77.
[37] Govender T, Stolnik S, Garnett MC, Illum L, Davis SS. PLGA nanoparticles prepared by nanoprecipitation: drug loading and release studies of a water soluble drug. J Control Release 1999;57(2):171–85.
[38] Lo CT, Van Tassel PR, Saltzman WM. Simultaneous release of multiple molecules from poly (lactide-co-glycolide) nanoparticles assembled onto medical devices. Biomaterials 2009;30(28):4889–97.
[39] Choi JS, Cao J, Naeem M, et al. Size-controlled biodegradable nanoparticles: preparation and size-dependent cellular uptake and tumor cell growth inhibition. Colloids Surf B Biointerfaces 2014;122:545–51.
[40] Danhier F, Ansorena E, Silva JM, Coco R, Le Breton A, Préat V. PLGA-based nanoparticles: an overview of biomedical applications. J Control Release 2012;161(2):505–22.
[41] Portlock JCalos M. Site-specific genomic strategies for gene therapy. Curr Opin Mol Ther 2003;5(4):376–82.
[42] Sim T, Lim C, Hoang NH, Oh KT. Recent advance of pH-sensitive nanocarriers targeting solid tumors. J Pharm Investig 2017;47(5):383–94.
[43] Kim CH, Lee SG, Kang MJ, Lee S, Choi YW. Surface modification of lipid-based nanocarriers for cancer cell-specific drug targeting. J Pharm Investig 2017;47(3):203–27.
[44] Wilhelm C, Billotey C, Roger J, Pons J, Bacri JC, Gazeau F. Intracellular uptake of anionic superparamagnetic nanoparticles as a function of their surface coating. Biomaterials 2003;24(6):1001–11.
[45] Yang PH, Sun X, Chiu JF, Sun H, He QY. Transferrin-mediated gold nanoparticle cellular uptake. Bioconjug Chem 2005;16(3):494–6.